Earth and Planetary Science Letters 403 (2014) 210–216

Contents lists available at ScienceDirect

Earth and Planetary Science Letters

www.elsevier.com/locate/epsl

Ball-and-socket tectonic rotation during the 2013 M_w7.7 Balochistan earthquake

W.D. Barnhart [a,*], G.P. Hayes [a], R.W. Briggs [a], R.D. Gold [a], R. Bilham [b]

[a] U.S. Geological Survey Geologic Hazards Science Center, Golden, CO 80401, USA

[b] Department of Geological Sciences and Cooperative Institute for Research in Environmental Sciences, University of Colorado, Boulder, CO 80309, USA

ARTICLE INFO

Article history:
Received 17 April 2014
Received in revised form 1 July 2014
Accepted 3 July 2014
Available online 24 July 2014
Editor: P. Shearer

Keywords:
geodesy
seismology
continental strike slip earthquakes
block rotations

ABSTRACT

The September 2013 M_w7.7 Balochistan earthquake ruptured a ~200-km-long segment of the curved Hoshab fault in southern Pakistan with 10 ± 0.2 m of peak sinistral and $\sim 1.7 \pm 0.8$ m of dip slip. This rupture is unusual because the fault dips $60 \pm 15°$ towards the focus of a small circle centered in northwest Pakistan, and, despite a 30° increase in obliquity along strike, the ratios of strike and dip slip remain relatively uniform. Surface displacements and geodetic and teleseismic source inversions quantify a bilateral rupture that propagated rapidly at shallow depths from a transtensional jog near the northern end of the rupture. Static friction prior to rupture was unusually weak ($\mu < 0.05$), and friction may have approached zero during dynamic rupture. Here we show that the inward-dipping Hoshab fault defines the northern rim of a structural unit in southeast Makran that rotates – akin to a 2-D ball-and-socket joint – counter-clockwise in response to India's penetration into the Eurasian plate. This rotation accounts for complexity in the Chaman fault system and, in principle, reduces seismic potential near Karachi; nonetheless, these findings highlight deficiencies in strong ground motion equations and tectonic models that invoke Anderson–Byerlee faulting predictions.

Published by Elsevier B.V.

1. Introduction

Dipping faults rarely slip in a strike-slip sense. Commonly, dipping faults accommodate convergence or extension whereas strike-slip displacements occur on nearly vertical faults. Where stresses are oblique to a system of dipping and vertical faults, slip is observed to be partitioned between them according to the relationships of Anderson–Byerlee fault mechanics (Anderson, 1972; Byerlee, 1978; Sibson, 1985; Jones and Wesnousky, 1992). The September 24, 2013 M_w7.7 Balochistan strike-slip earthquake is thus unusual in that it ruptured a 200+ km section of a curved reverse fault within the mechanically weak Makran accretionary prism of southern Pakistan (Fig. 1a). Despite fault dips of 45–75°, the earthquake slipped in a dominantly left-lateral sense (~6:1 SS:DS ratio). The plate boundary zone near the triple junction between the Eurasia, India, and Arabia (Ormara microplate) plates (Fig. 1a), location of the Balochistan earthquake, is characterized by east–west oriented reverse faults. These include the Panjgur, Hoshab, and Nai Rub fault system (PHNFS) where the traces swing counter-clockwise as they approach the India plate (Lawrence et al., 1981). This rotation results in a striking curved structural grain to the fold belt in southeast Balochistan. The transpressional India/Eurasia boundary to the east is defined by the Chaman fault system, represented at the latitude of the Balochistan earthquake by the left stepping discontinuous Ghazaband, and Ornach–Nal faults as it approaches the Makran triple junction. A sparse GPS network reveals relative motion between India and Eurasia at this latitude is accommodated by >2.5 cm/yr of sinistral shear and by at least 1.5 cm/yr of north–south shortening towards the Makran coast (Szeliga et al., 2012). India/Eurasia transform velocities near Karachi (population >23 million) are ~3.0 cm/yr. Historical seismicity in this region, particularly along the southern Ornach–Nal fault, over the past century is sparse (Ambraseys and Bilham, 2003), though several notable events include a series of moderate to large earthquakes on the Chaman fault system in the 1930s, including a May 1935 M7.5 event on the Ghazaband fault (Singh and Gupta, 1980). Similarly, an M8 earthquake in 1945 ruptured the Makran megathrust south of the Balochistan earthquake (Byrne et al., 1992). Despite its close proximity to the India/Eurasia plate boundary, no damaging earthquake has occurred near the megacity of Karachi (Bilham et al., 2007). However, there is some evidence to suggest than an earthquake circa 906 AD destroyed the ancient port of Bandhore, 40 km to the east of Karachi (Kovach et al., 2010).

* Corresponding author.
E-mail address: wbarnhart@usgs.gov (W.D. Barnhart).

http://dx.doi.org/10.1016/j.epsl.2014.07.001
0012-821X/Published by Elsevier B.V.

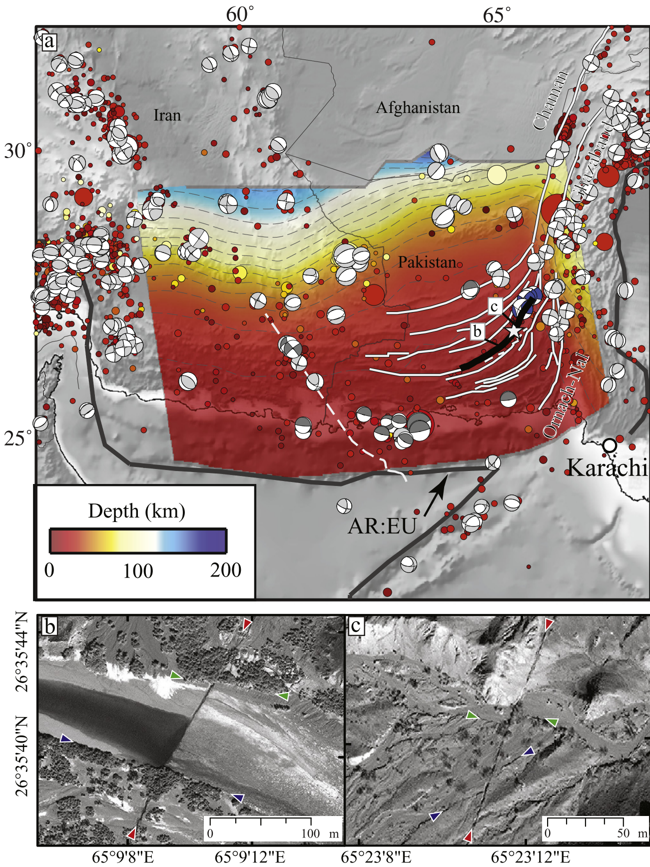

Fig. 1. (a) Tectonic setting of the Balochistan earthquake (white star). Historic seismicity from the USGS ComCat is shown colored by depth. Centroid moment tensors (light gray) from the gCMT catalog are plotted at USGS epicenters. Dark gray mechanisms are fault plane solutions from Byrne et al. (1992). Regional faults (white) are taken from Lawrence et al. (1981) and Szeliga et al. (2012). Major transform faults of the Chaman fault system are labeled. The thick black line shows the Landsat-interpreted surface rupture from the 2014 event. The dashed red and black line is the approximate location of the Sonne fault (Kukowski et al., 2000). The depth of the subducting Arabia (Ormara) slab is shown as a colored grid, with dashed gray contours every 10 km (beginning at 20 km), after (Hayes et al., 2012; Barnhart et al., 2014). Arabia:Eurasia (AR:EU) plate motions are shown by the black arrow (DeMets et al., 2010). Major plate boundaries are shown in dark gray. (b) and (c) High-resolution optical imagery (© DigitalGlobe, NextView license) showing left-lateral surface rupture associated with the Balochistan earthquake. Additionaly, (b) shows a northwest facing normal faulting scarp onto which water has ponded. Red triangles depict fault trace and blue and green triangles show left-laterally faulted stream margins and gullies. (For interpretation of the references to color in this figure legend, the reader is referred to the web version of this article.)

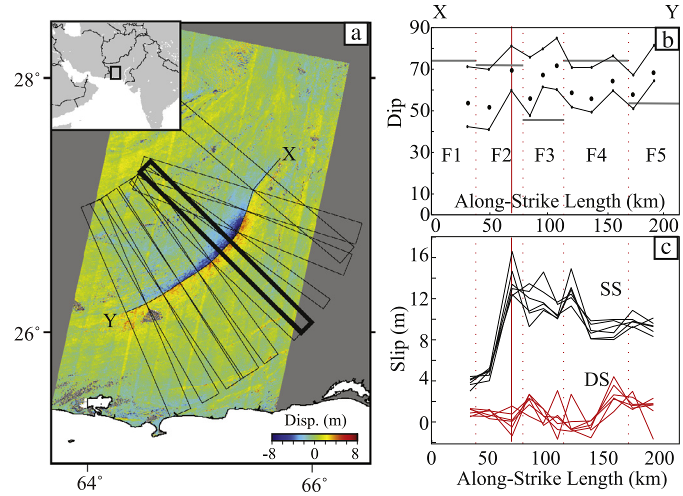

Fig. 2. (a) North–south displacements derived from Landsat-8 sub-pixel correlation and profiles used to invert for variations in fault geometry. Fault trace corresponds to the surface trace of the slip distributions shown in Fig. 3. Bolded profile is shown in Supplementary Fig. S3. Image-parallel stripes are an artifact of the "push-broom" sensor. (b) Best-fit dip and 1-sigma uncertainties of each profile in (a), plotted from north to south. Bins F1–F5 indicate the bounds of each constant-strike fault segment used geodetic and teleseismic modeling (Supplementary Table S1). All orientation uncertainties are in Table 1. Horizontal bars indicate the best-fit dip of each fault segment inferred from teleseismic observations. (c) Pure strike-slip and dip-slip components within each profile from geodetic slip and variable rake inversions. Each profile corresponds to one of the six fault geometries tested (Supplementary Table S1).

Several observations of earthquake rupture from seismology and remote sensing geodesy provide quantitative constraints of the rupture process of the Balochistan earthquake (e.g., Avouac et al., 2014; Jolivet et al., 2014). Centroid moment tensor (CMT) solutions from the U.S. Geological Survey (USGS, W-phase) and the global CMT project (Ekström et al., 2012) indicate that slip occurred in a left-lateral oblique sense at shallow depths (<20 km) on a moderately dipping structure (W-phase strike/dip/rake of 228°/45°/6°). Analysis of high-resolution WorldView2 satellite imagery confirms left-lateral surface rupture (Fig. 1b). Observations from normalized cross-correlation ("sub-pixel correlation" or "pixel tracking") of pre- and post-seismic Landsat-8 imagery show a nearly continuous, arcuate rupture that corresponds to slip along the Hoshab fault (Fig. 2a) (Lawrence et al., 1981; Avouac et al., 2014; Jolivet et al., 2014). We use these surface displacements to constrain variations in geometry of the rupture, slip direction, and the static slip distribution. We also use the spatial constraints from sub-pixel correlation to inform teleseismic finite source inversions for slip, fault geometry, and rupture velocity in order to provide a more detailed understanding of the kinematics of the Balochistan earthquake.

Previous studies of this earthquake (Avouac et al., 2014; Jolivet et al., 2014) have variably used Landsat-8 sub-pixel correlation results derived with COSI-Corr (Leprince et al., 2008), radar interferograms, teleseismic backprojection techniques, and teleseismic waveform inversion to explore the rupture characteristics of this event. These studies found a nearly continuous, arcuate fault rupture with shallow slip consistent with the results presented here. Furthermore, Avouac et al. (2014) and Jolivet et al. (2014) have noted the peculiar notion of nearly-pure strike-slip motion on a significantly dipping structure. Our modeling here expands on these previous studies to more explicitly define the fault geometry and constrain rupture kinematics, and we pose the existence of rigid block rotations within an accretionary prism. We also further demonstrate the efficacy of other sub-pixel correlation techniques (e.g., ampcor) to constrain surface displacements from optical imagery. Despite the differences in data sets, modeling approaches, and image processing techniques, the results of this and previous studies demonstrate remarkable consistency between earthquake source models – emphasizing the well-constrained rupture kinematics of the 2013 Balochistan earthquake.

2. Landsat-8 surface displacements

We perform sub-pixel correlation on pre- and post-seismic Landsat-8 Band 8 imagery (Sept. 10 2013–Sept. 26 2013, 15 m spatial resolution) to generate the surface displacement field of the Balochistan earthquake using the ampcor program included in the ROI_PAC interferometric synthetic aperture radar processing package (Fig. 2a) (Michel et al., 1999; Rosen et al., 2004). The two scene pairs shown are processed independently. Given the precision of the Landsat sub-pixel correlation results (~1.5 m, Supplementary Fig. S1) and that the post-seismic scene was acquired prior to the largest aftershock, we expect that the derived displacements dominantly reflect co-seismic displacements. The surface displacement results (spatial resolution = 60 m) show an arcuate, simple, and